Low-intensity illumination induced relaxation and charge transport behavior of single crystal halide perovskites

Avisek Maity,[1] Sudipta Chatterjee,[1] Barnali Ghosh,[1,*] and A. K. Raychaudhuri[2,†]

[1]*Department of Condensed Matter and Materials Physics, S. N. Bose National Centre for Basic Sciences, JD Block, Sector III, Salt Lake, Kolkata 700106, India*

[2]*CSIR Centre for Glass and Ceramic Research Institute, 196 Raja S.C. Mullick Road, Kolkata-700032, India*

(Received 6 April 2024; revised 28 June 2024; accepted 12 August 2024; published 23 August 2024)

We have investigated impedance, electric modulus, and dielectric spectroscopies, along with AC conductivity, on single crystals of methylammonium lead iodide (MAPI) and formamidinium lead iodide (FAPI) in the frequency range 50 Hz $\leqslant f \leqslant$ 1 MHz in the dark and under low-intensity illumination ($\leqslant$80 μW/cm^2). It is demonstrated that the relaxation observed in this frequency range in these single crystals can be attributed to space charge effects in the bulk of the crystals, which are caused by the finite time scale associated with charge relaxation, which can occur in this frequency range due to the large static dielectric constant and low conductivity of these solids. The relaxation was found to be faster in FAPI (with higher conductivity) compared to that in MAPI (with lower conductivity). The electron-hole pair generated by illumination enhances electronic conductivity and accelerates ionic migration by lowering the barrier; this, in turn, decreases the charge relaxation time and enhances the relaxation process. The barrier lowering inferred from the reduction in relaxation times by illumination is proposed to be associated with changes in the chemical potential attributed to carrier generation.

DOI: 10.1103/PhysRevMaterials.8.085404

I. INTRODUCTION

Perovskite halides with organic and inorganic cations at the A site have become one of the most intensively researched electronic materials over the last decade for photo voltaic and optoelectronic applications [1–5]. Solution processibility to make polycrystalline films, as well as single crystals at relatively lower temperatures (typically <200 °C), makes them attractive for low-cost electronic and optoelectronic devices [6]. To understand the performances of devices made by harnessing this class of materials and improve upon the performance parameters, investigations of the charge transport behavior are an essential requirement [7–9]. The charge transport mechanism in perovskite halides involves several important issues such as their ambipolar character (which includes similar contributions from ions and vacancies in addition to electron/hole contributions) and carrier coupling to phonons for polaron manifestations, to mention a few.

Various frequency (f) dependent techniques like ac conductivity ($\sigma_{ac}(f)$), complex impedance ($\tilde{Z}(\omega) = Z' + iZ''$, $\omega = 2\pi f$), modulus ($\tilde{M}(\omega) = M' + iM''$) and dielectric ($\tilde{\epsilon}(\omega) = \epsilon' + i\epsilon''$) spectroscopies have been extensively used to study the charge transport as well as dielectric relaxations in these materials [10–12]. These techniques done at a lower-frequency range ($f \leqslant$ 1 MHz) are of significance in the context of ionic migrations and relaxation processes associated with them, which can also be done under different external stimuli like temperature, pressure, and optical illumination [13,14].

Large ionic migrations in perovskite halides are facilitated by the presence of weak ionic and hydrogen bonds [15–17]. Consequently, the stability of the solar cells fabricated using these materials is largely dependent upon ionic migrations [18]. The concentrations of vacancies as well as those of organic cations and charged lead (Pb) and iodine (I) ions in these materials can be significantly higher than 10^{17} cm^{-3} [19]. Generally, it is believed that I^- ion is the most mobile species with a relatively larger diffusion coefficient $\sim 10^{-12}$ cm^{2}sec^{-1}. However, ionic migration can also occur by migration of charged mobile anion vacancies. The presence of such mobile species with varying mobility makes the issue of ionic migration challenging to understand which, in turn, has a direct impact on frequency-dependent relaxation that has been investigated in this manuscript.

Ionic migrations in perovskite halides (especially in 3D perovskite systems) depend on the interactions between the organic cations like methylammonium (MA^+) and formamidinium (FA^+) and the inorganic framework of PbI_6 cage. Substitution of organic cations can alter the bonding character of the Pb − I bonds, leading to observable electronic and optical properties [20]. In addition, the organic cations (MA^+ and FA^+) have dipole moments that are different in magnitudes and also in their natures [21]. It is thus expected that in perovskite halides, the organic cation in the A site could lead to differences in charge transport as well as the relaxation process among different cation-substituted perovskite halides both in the dark as well as under optical illumination. Illumination of the perovskite halides leads to enhanced ionic migration that occurs due to the lowering of the migration

*Contact author: barnali.ghoshsnb@gmail.com
†Contact author: arupraychaudhuri4217@googlemail.com

barrier under illumination [22,23]. This particular effect can affect the relaxation phenomena which have been probed in this paper. However, prolonged illumination of the perovskite halides with high intensity of illumination ($\geqslant$10 mW/cm^2) leads to irreversible structural changes that affect their optoelectronic properties, including decreasing efficiency of solar cells made from them [24,25]. High illumination intensity may lead to halide ion segregations in mixed-cation perovskite halides [26,27].

The relaxation times observed in different experiments like impedance, modulus, and dielectric spectroscopies in the frequency range (1 Hz−1 MHz), are typically in the range of milliseconds to microseconds [28,29]. This time scale is much slower than the time scales associated with some of the basic processes. For example, the time scales of molecular liberation and rotation are all faster than several picoseconds [30]. Relaxation due to dipole relaxations occurs at a frequency range in excess of 1 MHz and successive contributions from lattice vibrations and electronic contributions occur at even higher frequencies [31]. It has been suggested that the relaxation observed in the frequency range 1 Hz –1 MHz would arise from space charge (SC) effects [31,32]. The fundamental time constant of a system, known as charge relaxation time, is defined as

$$\tau_c = \frac{\epsilon}{\sigma_{\rm dc}}, \tag{1}$$

where $\epsilon = \epsilon_0 \cdot \epsilon_{\rm static}$, and ϵ_0 is the free space dielectric constant and $\epsilon_{\rm static}$ is the static dielectric constant and $\sigma_{\rm dc}$ is the dc conductivity. It would be important to explore if such SC relaxation in perovskite halides arises by or is related to this fundamental time constant.

Recently, studies on single crystals of perovskite halides and the devices that are made with them have increased significantly for different optoelectronic applications along with the investigation of fundamental properties like charge transport [33–37]. A large number of investigations in polycrystalline films of these materials using ac techniques as stated above along with ac conductivity has been reported [13]. However, extensive investigations of frequency-dependent relaxation studies involving single crystals (with and without illumination) have not been reported. In particular, there is a lack of such studies done under illumination to investigate the lowering of barriers to migration or shifts in relaxation frequencies. To the best of our knowledge, studies on the charge transport and relaxation behavior and its consequences on the optical response of perovskite halide single crystals with different organic cations (MA and FA) under optical illumination have not been reported before.

This paper presents impedance, modulus, dielectric, and ac conductivity measurements of perovskite halides $CH_3NH_3PbI_3$ (MAPI) and $CH(NH_2)_2PbI_3$ (FAPI) in the dark and under low-intensity illumination ($\leqslant$80 μW/cm^2) in the frequency range 50 Hz $\leqslant f \leqslant$ 1 MHz. Such a low illumination intensity is less than at least five orders that lead to irreversible sample degradation. This allows measurements to be done under illumination without being affected by the degradation phenomena. Our objective is to obtain the relaxation time (τ_A) from multiple experiments under dark and under illumination and to compare them with the fundamental

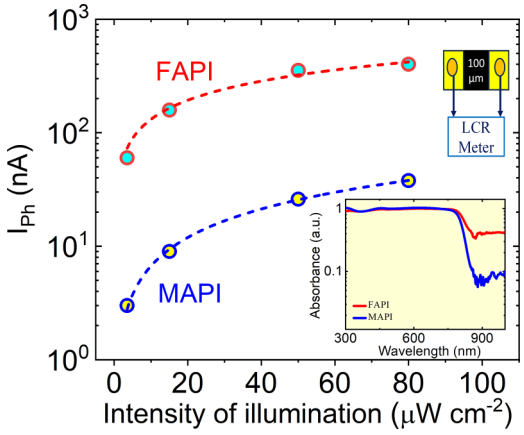

FIG. 1. Photocurrent ($I_{\rm Ph}$) as a function of illumination intensity P for MAPI and FAPI single crystals. The lines through the data represent the fit with the equation $I_{\rm Ph} = BP^{\gamma}$. The inset shows the schematic of the arrangement for electrical and optoelectronic measurements as well as the absorbance as a function of wavelength (λ).

charge relaxation time constant (τ_c) as previously defined. We have investigated the change in barrier height $\Delta\phi_A$ for a given relaxation process (A) that occurs under illumination. The subscript A refers to Z, M, and H for impedance spectroscopy, modulus spectroscopy, and the hopping process, respectively. We also observe that there are noticeable quantitative differences in the relaxation time-related parameters between the two crystals with different organic cations, namely MA and FA.

II. EXPERIMENTAL DETAILS

The experiments were carried out on single crystals of MAPI and FAPI which were grown from solution by the inverse temperature crystallization (ITC) method. The details of the crystal growth are given in previous publications from our group [38]. The as-grown crystals have a typical size of ∼3−5 mm in lateral dimensions and have a thickness ∼1−2 mm. The as-grown single crystals were characterized by photoluminescence (PL) spectroscopy, and absorbance spectroscopy for optical characterization as well as by x-ray diffraction (XRD) (see Figs. S1 and S2 of the Supplemental Material [39]).

Contacts on the flat faces of the crystals for electrical and optoelectronic measurements were made by thermal evaporation through a wire mask. The Cr/Au pads were used as electrodes. The electrical and optoelectronic measurements were done in an in-plane configuration as shown in the inset of Fig. 1 with a channel length of 100 μm. The optical image of the as-prepared sample with electrodes is shown in Fig. S3 of the Supplemental Material [39]. For DC as well as AC measurements the bias was kept ≈3 V so that the applied field is ∼0.03 V/μm. This is much less than the field that leads to polling [22]. The measurements were carried out in a chamber (with a Quartz window) that was pumped down to a vacuum better than 10^{-3} mbar. The chamber was purged a few times before evacuation with dry nitrogen gas.

The complex impedance $\tilde{Z}(f)$ in the dark as well as under illumination and the photoconductivity (PC)

measurements were performed using a xenon lamp source and a monochromator with an intensity of illumination ranging from 3.5 μW/cm^2 to 80 μW/cm^2, which is well below the illumination intensity used in most published papers that lead to irreversible ion migrations. The calibration of intensity was done using a calibrated silicon detector. A source meter was used for the DC electrical measurements like photoconductivity. The complex impedance measurement was done with the help of an LCR meter working in the frequency range of 50 Hz $< f <$ 1 MHz. Complex $\tilde{M}(f)$, $\tilde{\epsilon}(f)$ as well as AC conductivity were obtained from measured $\tilde{Z}(f)$.

III. RESULTS

A. Structural and optical characterization

The XRD shows that both the as-grown crystals of MAPI and FAPI are strongly textured along specific directions. The absorbance as a function of wavelength (λ) is shown in the lower inset of Fig. 1. It shows a sharp absorption edge and the absence of any substantial sub-bandgap absorption. From the absorption spectra, the band gaps were measured to be ≈1.53 eV for MAPI and ≈1.48 eV for FAPI. The PL spectra exhibit well-defined peaks near the band-edge wavelength (see Fig. S2 of [39]).

Figure 1 shows the result of photoconductivity measurements carried out on both of the single crystals. The photocurrent $I_{\rm Ph}(= I_{\rm ill} - I_d)$ is plotted in Fig. 1 as a function of illumination intensity (P). The $I_{\rm ill}$ and I_d are device currents under illumination and in the dark, respectively. $I_{\rm Ph}$ is observed to follow dependence on P that can be expressed as $I_{\rm Ph} = BP^{\gamma}$, where B and γ are constants. The values of the exponent γ as obtained from fit to the data (shown as the dashed line in Fig. 1) are ≈0.83 for MAPI and ≈0.56 for FAPI. Generally, the existence of trap states (near the conduction band minima and valence band maxima) and second-order charge recombination reduce the exponent γ to <1 [17,40]. The values of γ thus indicate the existence of trap states in the crystal near the band edges, which are more for FAPI than MAPI.

The photocurrent decay in MAPI demonstrates a higher rate of decay, with a time constant falling within the sub-one-second range. On the other hand, in FAPI, the photocurrent decays with two-time constants when illumination is turned off. There is one shorter time constant, which is ∼1 second, and another shorter time constant, which has a longer time constant of ∼10 seconds (see Fig. S4 of the Supplemental Material [39]) This behavior of long photocurrent decay in FAPI is expected to be related to the higher density of trap states near the band edges as noted by a smaller value of γ, as noted before.

In our experiment, the illumination intensity was ⩽80 μW/cm^2. This means that the response is reversible and does not exhibit any degradation when exposed to prolonged light. This is in contrast to the long-range migration of ions under illumination that has been reported when a much larger optical power is used [41,42]. This justifies the rationale of using low-intensity illumination so that effects arising from long-range ion migrations can be mitigated.

B. Impedance spectroscopy

Figures 2(a) and 2(c) show the variation of the imaginary part of the impedance (Z'') of MAPI and FAPI single crystals respectively, as a function of frequency f (from 50 Hz to 1 MHz) under different illumination at a wavelength λ = 800 nm, and at a bias of 3V. It can be clearly seen that there is one distinct relaxation peak in each of them. The peak value in Z'' is denoted as $Z''_{\rm max}$ which occurs at a frequency $f^Z_{\rm max}$. The relaxation time as obtained from the peaks is given as $\tau_z = \frac{1}{2\pi f^Z_{\rm max}}$. The values of τ_z for both MAPI and FAPI as a function of the intensity of illumination are shown in Fig. 3. Illumination reduces the maxima in the loss peaks and progressively shifts $f^Z_{\rm max}$ to higher values as the illumination intensity increases. This implies a progressive reduction of τ_z with illumination as shown in Fig. 3. The results we obtained are in general agreement with impedance spectroscopy data reported in MAPI single crystal [43], where they find that under the illumination of 10 mW/cm^2, τ_z = 198 microseconds, which decreases further to 82 microseconds with 100 mW/cm^2 illumination. A quantitative comparison with our results shows that the intensity dependence tapers off at a higher intensity of illumination.

The two materials with different cations (MA and FA) show distinctly different relaxation times. The value of $f^Z_{\rm max}$ (in the dark) is lower in MAPI by a factor of nearly 40 compared to that in FAPI, indicating that the relaxation process is much slower in MAPI. The real and imaginary part of impedance data for both MAPI and FAPI in the dark is shown in Fig. S6 of [39].

For MAPI, $f^Z_{\rm max}$ occurs at 1.3×10^2 Hz in the dark, which shifts by a factor of almost eight to ≈10^3 Hz under the illumination of 80 μW/cm^2. The illumination also reduces $Z''_{\rm max}$ by approximately four times. In the case of FAPI, the dependence of $f^Z_{\rm max}$ on illumination is comparatively weaker. For FAPI, $f^Z_{\rm max} = 5 \times 10^3$ Hz in the dark, which shifts to 1.5×10^4 Hz with a reduction in $Z''_{\rm max}$ by approximately 2.8.

The impedance data (at varying intensities of illumination) for both samples are depicted in conventional Nyquist plots as shown in Figs. 2(b) and 2(d) for MAPI and FAPI, respectively. The nearly semicircular shape of the curves indicates a single relaxation time with almost Debye-type relaxation. The real and imaginary parts of the impedance data are fitted to the following equation:

$$Z(\omega) = Z_\infty + \frac{Z_S - Z_\infty}{1 + (i\omega\tau_0)^\beta} \tag{2}$$

where Z(ω) is the complex impedance, $\omega = 2\pi f$, Z_S is the static impedance at $f \to 0$ and Z_∞ is the impedance at very high frequency (well beyond the relaxation frequencies), τ_0 is the relaxation time, and β is the stretched relaxation parameter, where $\beta = 1$ indicates conventional Debye relaxation with single relaxation time [44]. Figures 2(a) and 2(c) depict solid lines representing fit to the data. The parameter β as obtained from the fit of the data as a function of illumination intensity (at wavelength λ = 800 nm) for MAPI and FAPI crystals is shown in Fig. S7 of the Supplemental Material [39]. In dark conditions, the value of β for MAPI is 0.80 and that for FAPI is 0.95, implying that for FAPI the relaxation is more Debye-like. The fitted data in the dark for both MAPI

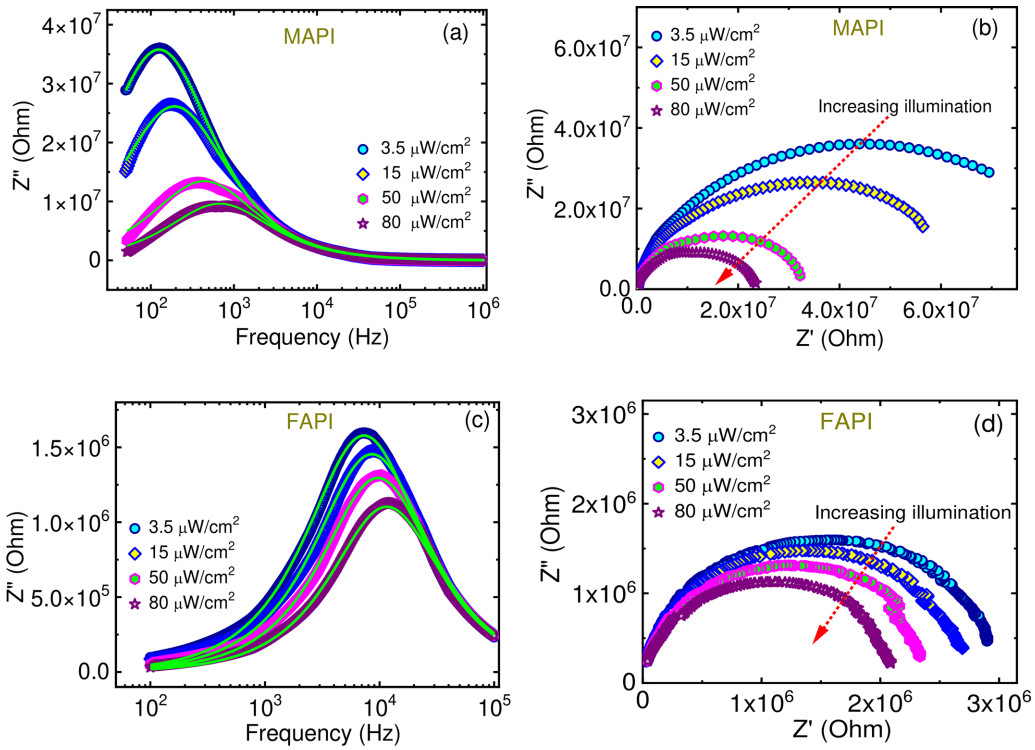

FIG. 2. Imaginary part of impedances (Z'') as a function of frequency (f) under different illumination intensities for (a) MAPI and (c) FAPI single crystals. The Nyquist plots for (b) MAPI and (d) FAPI are also shown. (The real part of the impedances under different illumination intensities for both the crystals is given in Fig. S5 of the Supplemental Material [39].)

and FAPI are shown in Fig. S6 [39]. Under illumination, the β value for MAPI increases with optical power and reaches 0.85, while for FAPI it reaches 1. This suggests that under illumination, the relaxation in both systems displays a more Debye-like behavior.

As depicted in Figs. 2(a) and 2(c), it can be observed that the impedances Z'' exhibit reduction in response to enhancement of the illumination intensity, for both MAPI and FAPI. At a frequency of 10^2 Hz, the decrease is comparable for both samples. The decrease under illumination at a lower frequency can mostly be ascribed to an increase in DC conductivity during illumination, as demonstrated subsequently. The impact of illumination diminishes as the frequencies increase. In the case of MAPI, this is observed at a frequency of $f \geqslant 5 \times 10^2$ Hz, while for FAPI, it is observed at $f \geqslant 10^4$ Hz.

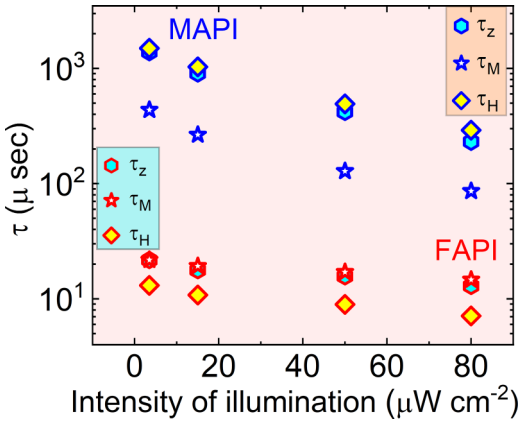

FIG. 3. Dependence of different relaxation times for the MAPI and FAPI single crystals as a function of illumination intensity as obtained from the data. τ_z, τ_M, and τ_H are obtained from the maxima in Z'', M'' and the hopping frequency, respectively.

C. Electric modulus spectroscopy

Combining electric modulus spectroscopy with impedance spectroscopy yields additional insights that can be utilized to derive significant inferences. The complex electric modulus $\tilde{M} = M' + iM''$ has been obtained from the complex impedance data ($\tilde{Z} = Z' + iZ''$) using the equations:

$$M'(f) = 2\pi f C_0 Z''(f), \quad M''(f) = 2\pi f C_0 Z'(f), \quad (3)$$

where C_0 is the free space capacitance. The data $M'(f)$ and $M''(f)$ are illustrated in Fig. 4 for both the samples as a function of frequency f for different values of the intensity of illumination. In both samples, the frequency $f^M_{\max}$ at which the maximum occurs in M'' is increased by increasing illumination intensity, which also raises the value of the M'' maxima. The impact of illumination is more pronounced in the case of MAPI compared to that in FAPI.

The values of $\tau_M = \frac{1}{2\pi f^M_{\max}}$ are displayed in Fig. 3. It is evident that τ_M and τ_z have nearly similar dependences on illumination intensity. In FAPI, the value of τ_M is approximately equal to τ_z, suggesting that the frequency of maxima in Z'' and M'' are the same, implying that the value of $f^Z_{\max} \approx f^M_{\max}$. While in MAPI, the ratio $\frac{\tau_Z}{\tau_M} \approx 3.2 - 3.4$ as the intensity of illumination varies and τ_Z is $>$ τ_M at all illumination intensities. This suggests that the frequencies at the maxima for

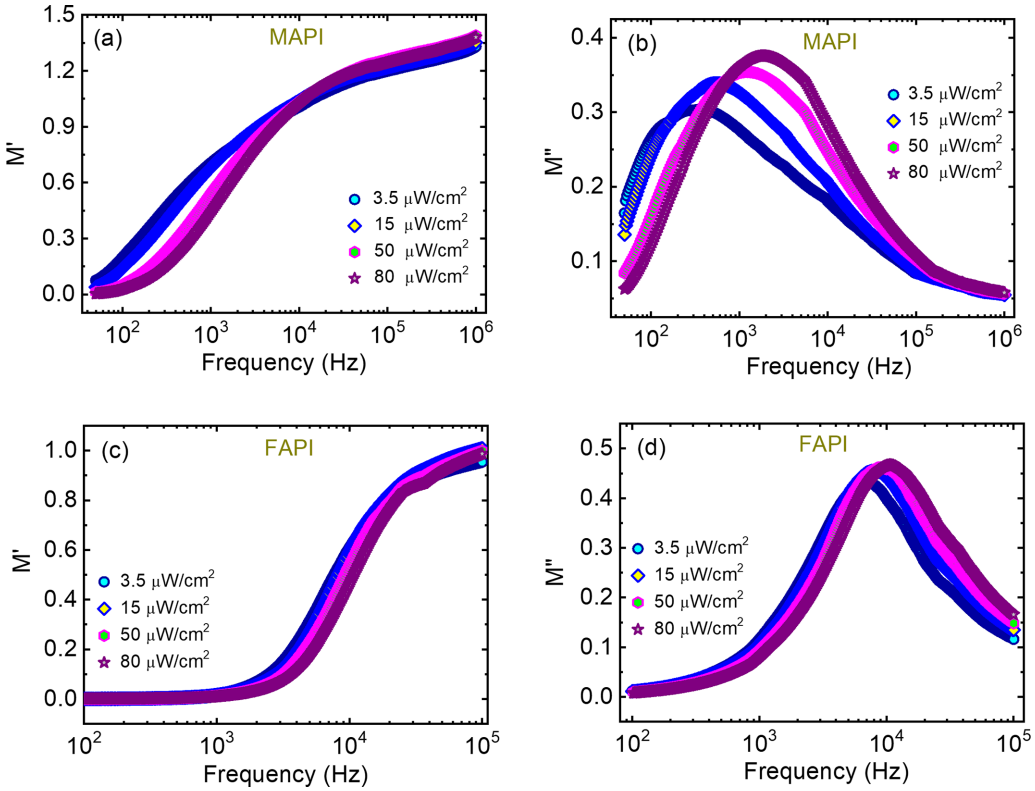

FIG. 4. Real (M') and imaginary (M'') parts of the electric modulus plotted as a function of frequency (f). [(a), (b)] MAPI and [(c), (d)] FAPI under different intensities of illumination.

Z'' and M'' do not coincide for MAPI, and $f^Z_{\max} < f^M_{\max}$. This observation allows us to reach an important inference stated below.

Following conventional wisdom [45], in FAPI, the overlapping of the peak frequencies of Z'' and M'' (i.e., $f^Z_{\max} \approx f^M_{\max}$) would imply that it has nonlocalized long-range ionic migration, giving rise to the conduction process and having higher conductivity. On the other hand, in MAPI, $f^Z_{\max} \neq f^M_{\max}$, suggesting that the carrier migration is localized as in a local dielectric relaxation. Importantly, these behaviors are retained under illumination. This observation will impact the conductivity process, which we will address in the next subsection. We have also obtained the frequency-dependent complex dielectric constant data ($\tilde{\epsilon}(f)$) from the measured $\tilde{Z}(f)$, which we have shown in Fig. S8 of the Supplemental Material [39].

D. ac conductivity

In Figs. 5(a) and 5(b) we have shown the AC conductivity ($\sigma_{\rm ac}(f)$) of MAPI and FAPI, respectively, as a function of frequency f for different illumination intensities. It can be seen that there are noticeable changes in the conductivity, in particular in the dc conductivity σ_0 as $f \to 0$. The conductivity data are fitted to the power law given as [46]:

$$\sigma_{\rm ac}(f) = \sigma_0\left[1 + \left(\frac{f}{f_H}\right)^n\right] \tag{4}$$

where σ_0 is the DC conductivity ($\sigma_{\rm dc}$), f_H is the hopping frequency, and n is the power law exponent that is generally interpreted as the crossover frequency from frequency-independent (DC conductivity) to the frequency-dependent dispersive region at higher frequency [46]. The fit to the data is also shown in Figs. 5(a) and 5(b) with solid lines. The frequency-dependent hopping term originates from ionic migration that occurs predominantly in the octahedral sites that contain the Pb and I ions and their vacancies as well. The parameters f_H and $\sigma_{\rm dc}$ as obtained from the fit are shown in Figs. 5(c) and 5(d), respectively. We also define a hopping time constant $\tau_H = \frac{1}{2\pi f_H}$, which are shown in Fig. 3 along with the other time constants. This shows that like other time constants, τ_H is also lowered by illumination.

It is also noteworthy that there are qualitative differences between MAPI and FAPI regarding the interrelations of the different time constants obtained from the experimental parameters as shown in Fig. 3. For all the processes, FAPI has much smaller time constants (signifying a faster relaxation process) compared to those of MAPI. The higher value of f_H for FAPI compared to that for MAPI can also be seen in Figs. 5(a) and 5(b) where the frequency-independent region for $\sigma_{\rm ac}$ persists to a much higher frequency range in FAPI. The frequency-dependent AC conductivity in the dark is given in Fig. S9 [39].

The qualitative differences in the relaxation parameters between the two materials remain unaltered even under illumination, although all the time constants are shortened, showing faster relaxation processes under illumination even at a very low intensity ($\leqslant 80\ \mu W/cm^2$). The effect of illumination on the hopping frequency f_H is also substantial for MAPI where it is enhanced by a factor of $\sim$5 compared to an enhancement by a factor of only $\sim$2.9 for FAPI. The exponent

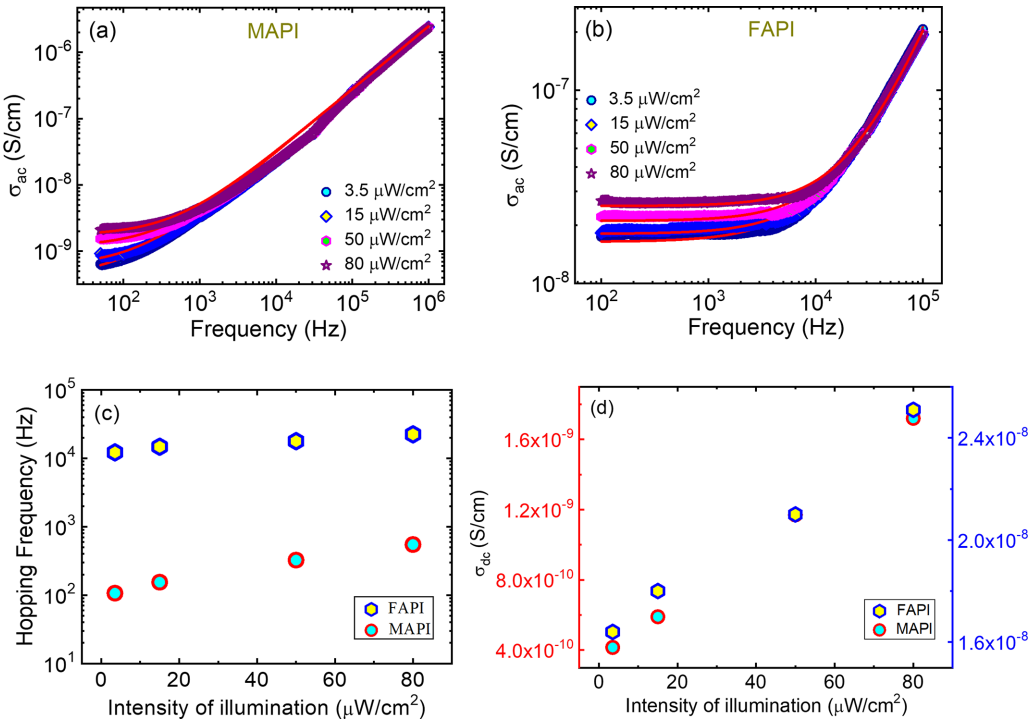

FIG. 5. Frequency dependence of ac conductivity(σ_{ac}) for (a) MAPI and (b) FAPI single crystals under different intensities of illumination. (c) Hopping Frequency (f_H) and (d) dc conductivity (σ_{dc}) as a function of illumination intensity for MAPI and FAPI crystals.

n in the dark and under illumination stays close to the range 0.9–1.0, showing a shallow variation with intensity. In MAPI, $\tau_H \approx \tau_Z > \tau_M$. However, in FAPI the relative orders change, where $\tau_H < \tau_Z \approx \tau_M$. This reflects a basic difference in the relaxation process in the two materials.

As can be seen in Fig. 5(d), MAPI has a much less σ_{dc} compared to that of FAPI by a factor of ≈40 at the lowest light intensity. This is in conformity with the real value of impedance Z' as $f \to 0$, which is higher in MAPI compared to that in FAPI. The enhancement of σ_{dc} as a function of illumination is more prominent in MAPI where it is enhanced by a factor of nearly four when the intensity is enhanced by a factor of ≈23. For FAPI the enhancement of σ_{dc} is only by a factor of ≈1.5 for the same intensity of illumination variation.

To summarize the important observations on the dependence of cations, we find that the MAPI has lower DC conductivity, larger impedance, and a comparatively slower relaxation (i.e., larger τ_Z and τ_M) in the frequency range investigated compared to those in FAPI. MAPI also shows a more prominent dependence of the relaxation parameters on the illumination intensity compared to those of FAPI under the same illumination intensity. There are also important differences in the relative values of the different time constants. In MAPI, τ_H overlaps with τ_Z and is the largest time constant larger than τ_M. In contrast, in FAPI, τ_H is the shortest time constant smaller than both τ_Z and τ_M which are overlapping.

IV. DISCUSSIONS

A. Origin of relaxation in MAPI and FAPI for f ⩽ 1 MHz

As previously stated, relaxations in the sub-1 MHz frequency range can likely be attributed to SC effects. In polycrystalline films such SC, effects can occur at the grain boundaries, at any chemical inhomogeneity, or contacts. Such SC effects can also happen at the interfaces of single crystals that lack homogeneities or have grain boundaries. Another important source of SC in a solid is local charge imbalances caused by a finite time scale of measurement, when the measurement time scale is faster than or comparable to the charge relaxation time τ_c described in Eq. (1) in the introduction. We demonstrate that the large static dielectric constant ϵ_{stat} in these materials can result in τ_c being very large. We also show that this scale is similar to or comparable with the different relaxation times observed in impedance, modulus, and dielectric spectroscopies, as well as the hopping time observed in ac conductivity.

To obtain the value of the charge relaxation time τ_c, one needs the value of ϵ_{static}. Taking a cue from published experimental data as well as theoretical evaluations [47], we use $\epsilon_{static} = \epsilon_{electronic} + \epsilon_{ion}$. The values of τ_c evaluated using the corresponding value of ϵ_{static} and σ_{dc} [see Eq. (1)] for both MAPI and FAPI in the dark and under illumination at the highest intensity used. These are shown in Table I. As can be seen from Table I, for MAPI $\tau_c = 6.25$ msec in the dark and under illumination the corresponding value is 1.58 msec. For FAPI, the values are 0.243 msec in the dark and 0.161 msec under illumination. The reduction in τ_c occurs due to enhancement in the DC conductivity σ_{dc} under illumination.

It can be seen that the relaxation times τ_A's along with the charge relaxation time τ_c decrease progressively as the intensity of illumination is increased. This is shown in Fig. 3 and the data are collected in Table II. We would like to explore how the τ_A's under dark and under illumination compare with the time scale set up by the τ_c. This is done by scaling τ_A's

TABLE I. Charge relaxation time τ_c in the dark and under illumination and intercomparison with experimental time scales τ_A's. D = In the dark, I = Under Illumination (intensity 80 μW/cm^2), ϵ_{static} from Ref. [47].

Sample	ϵ_{static}	τ_c(D) msec	τ_c(I) msec	$\frac{\tau_Z}{\tau_c}$(D)	$\frac{\tau_Z}{\tau_c}$(I)	$\frac{\tau_M}{\tau_c}$(D)	$\frac{\tau_M}{\tau_c}$(I)	$\frac{\tau_H}{\tau_c}$(D)	$\frac{\tau_H}{\tau_c}$(I)
MAPI	$\epsilon_{\text{static}} = 30.5$	6.52	1.58	0.25	0.15	0.07	0.06	0.23	0.19
FAPI	$\epsilon_{\text{staic}} = 45.0$	0.243	0.161	0.09	0.08	0.09	0.08	0.05	0.04

by τ_c and intercomparing the ratios $\frac{\tau_A}{\tau_c}$ for different A's. This can be seen in Table I. The relevant ratios for MAPI in the dark are 0.25 and 0.07, respectively, for $\frac{\tau_Z}{\tau_c}$ and $\frac{\tau_M}{\tau_c}$. (For MAPI, $\tau_H \approx \tau_Z$.) Under illumination, the corresponding ratios are 0.15 and 0.06, respectively. For FAPI in the dark, $\frac{\tau_Z}{\tau_c} = 0.09$ and $\frac{\tau_H}{\tau_c} = 0.05$. (For FAPI, $\tau_M \approx \tau_Z$.) The corresponding ratios under illumination are 0.08 and 0.04, respectively.

We find that the important time scale τ_c lies within an order or so of the values of all the relaxation and hopping times in the system. Thus, whatever the relaxation or hopping process, it occurs in the time scale of the charge relaxation that preserves local charge neutrality. This is also preserved under illumination (as can be seen in Table I and discussed later on). This observation of a quantitative similarity of τ_c with the other relaxation times in the sub-1 MHz region strongly suggests that the origin of the SC effect in single crystals can indeed arise from the finite value of τ_c.

In this proposed scenario, the higher frequency of relaxation or shorter time scales of relaxation (τ_A, $A = Z, M$) as well as a shorter hopping time τ_H in FAPI compared to those of MAPI, arise principally from a larger value of σ_{dc} of FAPI, which makes the charge relaxation faster. (The two solids have comparable ϵ_{static}). On illumination, the charge relaxation process becomes faster due to the reduction of τ_c arising from the enhancement of σ_{dc} on illumination [see Eq. (1)]. This makes the relaxation process faster thus reducing all the relevant τ_A's on illumination (see Fig. 3).

B. Lowering of the barrier under illumination

One of the important observations in this investigation is the reduction of all the relaxation times(τ_Z, τ_M), the hopping time constant τ_H as well as the DC conductivity σ_{dc} as the intensity of illumination is enhanced. It has been reported before in MAPI single crystals that the activation energy, derived from the temperature dependence of σ_{dc} is significantly lowered on illumination with intensity 25 mW/cm^2 [22]. The barrier lowering has been seen in thermally activated conduction for both MAPI and FAPI single crystals [23] with illumination intensity $P \sim$ 20–25 mW/cm^2. The reduction of the time constants on increasing the intensity of illumination (as observed in the present investigation) clearly suggests that there is a lowering of barrier height ϕ_A (related to a particular process A) associated with a given process on illumination. (We refer to the barrier for τ_Z as ϕ_Z, that for τ_H as ϕ_H, for τ_M as ϕ_M and for σ_{dc} as ϕ_σ.) As suggested in the previous subsection, we have associated the charge relaxation time τ_c with all the other relaxation time τ_A. Since τ_c is $\propto \sigma_{\text{dc}}^{-1}$, it is expected that the barrier lowering on the illumination of all the time constants τ_A's should be similar. This can be argued as support to the hypothesis that the observed relaxation arises from the finite values of charge relaxation times in these single crystals. We investigate this below. We propose to find out the extent of lowering a barrier as a function of illumination intensity (P) quantified through a parameter α_A (with unit $\frac{\text{meV}}{\mu\text{Wcm}^{-2}}$) assuming a linear relation at low intensity:

$$\phi_A = \phi_{0,A} - \alpha_A P \tag{5}$$

where $\phi_{0,A}$ is the barrier in the dark for a given process A. α_A is the coefficient of lowering that can be obtained from the experimental fit to the data. For any physical parameter with an activated process following the Arrhenius law, like the τ_Z, τ_M, and τ_H, this can be written as:

$$\tau_A(P) = \tau_{0,A} e^{\beta(\phi_{0,A} - \alpha_A P)} \tag{6}$$

where $\beta = \frac{1}{k_B T}$, k_B being the Boltzmann constant. $\phi_{0,A}$ being the barrier in the dark. The proposed linear reduction in ϕ_A by illumination as shown in Eq. (5), is valid for low values of P and the dependence on P may taper off at higher intensities. From the collage of data shown in Fig. 3, which is in a semi-log plot, for both MAPI and FAPI it can be seen that the τ_Z, τ_M, and τ_H follow a relation on P as shown in Eqs. 5 and 6. The values of different α_A's are shown in Table II for both MAPI and FAPI single crystals. It can be seen that for MAPI all the α_A's are very close and has an average value of $\approx$0.56 meV/μW cm^{-2}. For FAPI, there is a small variation ($\sim \pm$ 15%) in values of α_A derived from different τ_A's. It is lowest $\approx$0.13 for α_M, highest $\approx$0.19 for α_H, and the value is close to the average of $\approx$0.16. The lower value of α_A's for FAPI reflects shallower dependence of the σ_{dc} on the intensity of illumination [see Figs. 5(b) and 5(d)].

We have also calculated α_A using published data on MAPI single crystal [22] where the lowering of the barrier for activated conduction has been measured with an illumination

TABLE II. Illumination dependence of experimental time scales τ_A's and coefficient of barrier lowering α_A: D = In the dark, I = Under Illumination (intensity 80 μW/cm^2), τ_A's in msec and Unit of α_A in $\frac{\text{meV}}{\mu\text{W.cm}^{-2}}$.

Sample	τ_Z(D)	τ_Z(I)	α_Z	τ_M(D)	τ_M(I)	α_M	τ_H(D)	τ_H(I)	α_H
MAPI	1.595	0.231	0.58	0.435	0.086	0.56	1.49	0.29	0.54
FAPI	0.022	0.013	0.15	0.022	0.014	0.13	0.013	0.007	0.19

intensity of 25 mW/cm^2. This experiment used the same planar device as ours with similar symmetric Au contacts. The estimated coefficient obtained from the above-mentioned data is $\alpha_A = 0.023$ meV/μW cm^{-2}. This is much lower than $\alpha_A = 0.56$ meV/μW cm^{-2} observed by us for a much lower intensity of illumination. The lower value of α_A's estimated from that measured with a much larger intensity of illumination intensity (25 mW/cm^2) points to the fact that the dependence of the barrier on intensity tapers off for higher values of P, that are nearly three orders larger than that used by us.

At the highest intensity used by us (80 μW/cm^2) the barrier lowering $\Delta\phi_A(P)(=\phi_{A,P}\text{-}\phi_{A,0})$ is ≈40 meV for MAPI and 8–10 meV for FAPI. It is interesting that such a small lowering of the barrier can cause a clear observable effect. Similar values of the barrier lowering with illumination for all the different τ_A's support our hypothesis that these time scales are related to the same process, which we propose to be the fundamental charge relaxation process that has a time scale τ_c associated with it.

C. Ambipolar transport and effect of illumination

As stated in the introduction, charge transport in perovskite halides like MAPI and FAPI are ambipolar and can have contributions from both ions and electrons, so that $\sigma = \sigma_{\text{ion}} + \sigma_{\text{el}}$, where the subscripts refer to ionic and electronic conductivity respectively. Ionic conductivity is often thermally activated with an activation energy ϕ_σ and it is governed by the Arrhenius Law:

$$\sigma(T) = \sigma^* e^{\left(\frac{-\phi_\sigma}{k_B T}\right)}, \tag{7}$$

where σ^* is the pre-exponential factor. The ion transport can be high in these ambipolar materials so that $\sigma_{\text{ion}} \approx \sigma_{\text{el}}$ [48]. It has been argued that the illumination-induced enhancement of ionic migration can arise due to the ambipolar nature of transport. It has been proposed that in the presence of a larger density of photogenerated carriers on illumination, the photoconductivity is enhanced, leading to mitigation of the SC effect and allowing enhanced ionic migration.

On illumination, the observed σ_{dc} is enhanced, which happens due to enhancements of both the electronic and ionic contributions. The electronic contribution is enhanced due to electron-hole pair production on illumination (i.e., enhancement in carrier density) and the ionic contribution can be enhanced by lowering the activation barrier to ionic migration [22,23,42]. In our investigation, we find that for the highest intensity of illumination used by us, the observed σ_{dc} is enhanced by a factor of ∼4.2 for MAPI and by a factor of ∼1.53 for FAPI. The enhancements are small, given the low intensity of illumination that we use.

We would use certain plausible assumptions to separate the contributions of both the processes (electronic and ionic) in enhancing σ_{dc} under illumination. We assume that in the dark $\sigma_{\text{ion}} \approx \sigma_{\text{el}}$ as observed by several researchers [48] and the second assumption is that the enhancement of σ_{ion} on illumination occurs primarily due to the lowering of the barrier $\Delta\phi_A$, which we can estimate from the relaxation time data as discussed in the previous subsection. The brief procedure that we followed is described below.

The ratio of σ_{dc} under dark (sub-script d) and under illumination (sub-script ill) at the highest intensity used (80 μW cm^{-2}) can be written as:

$$\frac{(\sigma_{\text{dc}})_{\text{ill}}}{(\sigma_{\text{dc}})_d} = \frac{(\sigma_{\text{ion}})_{\text{ill}}}{2(\sigma_{\text{ion}})_d} + \frac{(\sigma_{\text{el}})_{\text{ill}}}{2(\sigma_{\text{el}})_d}, \tag{8}$$

where we used the assumption that in the dark $(\sigma_{\text{ion}})_d \approx (\sigma_{\text{el}})_d \approx \frac{1}{2}(\sigma_{\text{dc}})_d$. The ratio of σ_{ion} under dark and illumination can be related by

$$\frac{(\sigma_{\text{ion}})_{\text{ill}}}{(\sigma_{\text{ion}})_d} = e^{\beta\Delta\phi_\sigma}. \tag{9}$$

The value of the lowering of barrier $\Delta\phi_\sigma$ is evaluated for the highest intensity of illumination. We use the lowering of barrier as observed for the hopping process so that $\Delta\phi_\sigma = \Delta_H$. From these values, we obtain $\frac{(\sigma_{\text{ion}})_{\text{ill}}}{(\sigma_{\text{ion}})_d} \approx 5.64$ for MAPI and 1.58 for FAPI. Using these values we obtain from Eq. (8) the ratio $\frac{(\sigma_{\text{el}})_{\text{ill}}}{(\sigma_{\text{el}})_d} \approx 2.7$ for MAPI and 1.5 for FAPI. It thus appears that under illumination the relative contributions to σ_{dc} from ions and electrons for FAPI remain unchanged under illumination. However, in MAPI the illumination enhances the relative contribution of ions to the σ_{dc}, mainly arising from the lowering of the barrier by illumination.

D. Change in chemical potential on illumination

The electron-hole pair generation leads to the enhancement of the σ_{el}. This lowers the charge relaxation time, reduces the SC effects, and in turn enhances ionic migration. Electron/hole transport as well as ionic transport in these materials are thus coupled. The ionic migration being activated, the enhancement of the migration by illumination thus can be interpreted as illumination-enabled lowering of the barrier as has been observed in the experiment.

In this scenario (i.e., lowering of activation barrier by illumination), a very important energy scale that would have an influence on the energy scales of barrier lowering is the change of the chemical potential $|\delta\psi|$ due to a change in carrier concentration on electron-hole pair generation on illumination. Change in chemical potential$|\delta\psi|$ due to change in carrier concentration is given by the relation

$$|\delta\psi| = \frac{k_B T}{e} \ln\left(\frac{n_{0+\delta n}}{n_0}\right), \tag{10}$$

where n_o is the carrier concentration in the dark and $n_0 + \delta_n$ is the carrier concentration under illumination, δ_n being the excess carrier concentration due to illumination. Assuming no change in mobility μ on illumination and using the relation $\sigma = n_c e\mu$, where n_c is the carrier concentration, we can relate the relative change in carrier concentration to the electronic conductivity change under illumination as: $(\frac{n_{0+\delta n}}{n_0}) \approx \frac{(\sigma_{\text{el}})_{\text{ill}}}{(\sigma_{\text{el}})_d}$. The ratio $\frac{(\sigma_{\text{el}})_{\text{ill}}}{(\sigma_{\text{el}})_d}$ has been estimated in the last subsection as being equal to 2.7 for MAPI and 1.5 for FAPI for the highest illumination used. Using these values we obtain $|\delta\psi| =$ 25.7 meV and 10.7 meV for MAPI and FAPI, respectively. This compares very well with the value of barrier lowering $|\Delta\phi_A| \approx 12$ meV for FAPI. However, for MAPI $|\delta\psi|$ is of the same order but less than $|\Delta\phi_A| \approx 40$ meV. In view of the approximations made for the calculation of the ratio $\frac{(\sigma_{\text{el}})_{\text{ill}}}{(\sigma_{\text{el}})_d}$, this

level of agreement may be considered reasonable. It is thus interesting that the scale of barrier lowering on illumination is similar to (or comparable) the scale of lowering of the chemical potential created by the excess carriers generated by the illumination.

V. CONCLUSIONS

The present investigation shows that in the frequency range $f \leqslant 1\,\mathrm{MHz}$ in perovskite halide single crystals like MAPI and FAPI, the observed relaxation phenomena can arise from space charge relaxation which is determined by the charge relaxation time τ_c defined by the conductivity and the static dielectric constant. For experimental measurements times smaller than τ_c, the unrelaxed charge excess leads to space charge which obstructs ionic migration. For longer measurement times, the charge relaxation leads to mitigation of space charge and this leads to faster ionic migration. The larger conductivity of FAPI leads to faster relaxation in this material compared to that in MAPI. It is observed that even a low-intensity illumination ($\leqslant 80\ \mu\mathrm{W/cm^2}$) makes the relaxation noticeably faster, which we suggest to originate from enhancement of conductivity (σ_{dc}) due to illumination and reduction of τ_c ($\propto \sigma_{\mathrm{dc}}^{-1}$). The enhancement of σ_{dc} on illumination originates from the lowering of the activation barrier, which we suggest arises from electron-hole pairs created by illumination.

ACKNOWLEDGMENTS

A.M. and S.C. thank S.N. Bose National Centre for Basic Sciences (SNBNCBS) for the fellowship. A.M acknowledges Dr. Pulak Pal for fruitful discussion. A.K.R. acknowledges financial support from the Science and Engineering Research Board (SERB), Government of India, as SERB Distinguished Fellow (File Number: SB/DF/008/2019. B.G. acknowledges the use of the Technical Research Centre (TRC) instrument facilities of SNBNCBS established under the TRC project of the Department of Science and Technology (DST), Government of India.

[1] J. S. Manser, J. A. Christians, and P. V. Kamat, Chem. Rev. **116**, 12956 (2016).
[2] Y. Zhao and K. Zhu, Chem. Soc. Rev. **45**, 655 (2016).
[3] A. K. Jena, A. Kulkarni, and T. Miyasaka, Chem. Rev. **119**, 3036 (2019).
[4] X.-K. Liu, W. Xu, S. Bai, Y. Jin, J. Wang, R. H. Friend, and F. Gao, Nat. Mater. **20**, 10 (2021).
[5] Z. Wang, S. Shu, X. Wei, R. Liang, S. Ke, L. Shu, and G. Catalan, Phys. Rev. Lett. **132**, 086902 (2024).
[6] H. Dong, C. Ran, W. Gao, M. Li, Y. Xia, and W. Huang, eLight **3**, 3 (2023).
[7] W. Tress, J. Phys. Chem. Lett. **8**, 3106 (2017).
[8] D. Ghosh, E. Welch, A. J. Neukirch, A. Zakhidov, and S. Tretiak, J. Phys. Chem. Lett. **11**, 3271 (2020).
[9] M. Zhang, X. Zhang, L.-Y. Huang, H.-Q. Lin, and G. Lu, Phys. Rev. B **96**, 195203 (2017).
[10] Q. Sun, X. Zhang, C. Zhao, W. Tian, and S. Jin, J. Phys. Chem. C **127**, 22868 (2023).
[11] A. Sahoo, T. Paul, P. Pal, N. H. Makani, A. Ghosh, and R. Banerjee, Phys. Rev. Appl. **20**, 034024 (2023).
[12] S. Mandal and A. Ghosh, J. Phys.: Condens. Matter **8**, 829 (1996).
[13] E. von Hauff and D. Klotz, J. Mater. Chem. C **10**, 742 (2022).
[14] D. Pitarch-Tena, T. T. Ngo, M. Vallés-Pelarda, T. Pauporté, and I. Mora-Sero, ACS Energy Lett. **3**, 1044 (2018).
[15] I. C. Smith, E. T. Hoke, D. Solis-Ibarra, M. D. McGehee, and H. I. Karunadasa, Angew. Chem. Int. Ed. **53**, 11232 (2014).
[16] C. Eames, J. M. Frost, P. R. Barnes, B. C. O'regan, A. Walsh, and M. S. Islam, Nat. Commun. **6**, 7497 (2015).
[17] S. D. Stranks, V. M. Burlakov, T. Leijtens, J. M. Ball, A. Goriely, and H. J. Snaith, Phys. Rev. Appl. **2**, 034007 (2014).
[18] A. Pockett, G. E. Eperon, N. Sakai, H. J. Snaith, L. M. Peter, and P. J. Cameron, Phys. Chem. Chem. Phys. **19**, 5959 (2017).
[19] A. Walsh, D. O. Scanlon, S. Chen, X. Gong, and S.-H. Wei, Angew. Chem. **127**, 1811 (2015).
[20] A. Amat, E. Mosconi, E. Ronca, C. Quarti, P. Umari, M. K. Nazeeruddin, M. Grätzel, and F. D. Angelis, Nano Lett. **14**, 3608 (2014).
[21] S. Liu, R. Guo, and F. Xie, Mater. Des. **221**, 110951 (2022).
[22] J. Xing, Q. Wang, Q. Dong, Y. Yuan, Y. Fang, and J. Huang, Phys. Chem. Chem. Phys. **18**, 30484 (2016).
[23] Y.-C. Zhao, W.-K. Zhou, X. Zhou, K.-H. Liu, D.-P. Yu, and Q. Zhao, Light Sci. Appl. **6**, e16243 (2017).
[24] H. Tsai, R. Asadpour, J.-C. Blancon, C. C. Stoumpos, O. Durand, J. W. Strzalka, B. Chen, R. Verduzco, P. M. Ajayan, S. Tretiak *et al.*, Science **360**, 67 (2018).
[25] D. d. Quilettes, S. Vorpahl, S. Stranks, H. Nagaoka, G. Eperon, M. Ziffer, H. Snaith, and D. Ginger, Science **348**, 683 (2015).
[26] Y. Zhao, P. Miao, J. Elia, H. Hu, X. Wang, T. Heumueller, Y. Hou, G. J. Matt, A. Osvet, Y.-T. Chen *et al.*, Nat. Commun. **11**, 6328 (2020).
[27] P. S. Mathew, G. F. Samu, C. Jan'aky, and P. Kamat, ACS Energy Lett. **5**, 1872 (2020).
[28] M. Javed, A. A. Khan, M. N. Khan, J. Kazmi, and M. A. Mohamed, Mater. Sci. Eng.: B **269**, 115168 (2021).
[29] N. H. Makani, A. Sahoo, P. Pal, T. Paul, L. S. Tanwar, M. Singh, A. Ghosh, and R. Banerjee, Phys. Rev. Mater. **6**, 115002 (2022).
[30] J. M. Frost and A. Walsh, Acc. Chem. Res. **49**, 528 (2016).
[31] J. N. Wilson, J. M. Frost, S. K. Wallace, and A. Walsh, APL Mater. **7**, 010901 (2019).
[32] K. Wu, Y. Huang, J. Li, and S. Li, Appl. Phys. Lett. **111**, 042902 (2017).
[33] B. Murali, H. K. Kolli, J. Yin, R. Ketavath, O. M. Bakr, and O. F. Mohammed, ACS Mater. Lett. **2**, 184 (2020).

[34] Y. Cho, H. R. Jung, and W. Jo, Nanoscale **14**, 9248 (2022).
[35] A. Maity, S. Chatterjee, A. K. Raychaudhuri, and B. Ghosh, ACS Appl. Electron. Mater. **4**, 4298 (2022).
[36] A. Kalam, R. Runjhun, A. Mahapatra, M. M. Tavakoli, S. Trivedi, H. Tavakoli Dastjerdi, P. Kumar, J. Lewiński, M. Pandey, D. Prochowicz *et al.*, J. Phys. Chem. C **124**, 3496 (2020).
[37] A. Mahapatra, R. Runjhun, J. Nawrocki, J. Lewiński, A. Kalam, P. Kumar, S. Trivedi, M. M. Tavakoli, D. Prochowicz, and P. Yadav, Phys. Chem. Chem. Phys. **22**, 11467 (2020).
[38] A. Maity, C. Das, A. Raychaudhuri, A. Saha, and B. Ghosh, J. Phys. D **54**, 455104 (2021).
[39] See Supplemental Material at http://link.aps.org/supplemental/10.1103/PhysRevMaterials.8.085404 for details of sample characterization and additional impedance spectroscopy data.
[40] R. H. Bube, *Photoelectronic properties of semiconductors* (Cambridge University Press, Cambridge, 1992).
[41] S. Ruan, M.-A. Surmiak, Y. Ruan, D. P. McMeekin, H. Ebendorff-Heidepriem, Y.-B. Cheng, J. Lu, and C. R. McNeill, J. Mater. Chem. C **7**, 9326 (2019).
[42] A. D. Marshall, J. Acharya, G. Alkhalifah, B. Kattel, W.-L. Chan, and J. Z. Wu, ACS Appl. Mater. Interfaces **13**, 33609 (2021).
[43] Q. Dong, Y. Fang, Y. Shao, P. Mulligan, J. Qiu, L. Cao, and J. Huang, Science **347**, 967 (2015).
[44] P. Debye, *Polar Molecules* (The Chemical Company, Inc., New York, 1929), Sec. 18, pp. 89–95.
[45] R. Gerhardt, J. Phys. Chem. Solids **55**, 1491 (1994).
[46] D. Almond and A. West, Nature (London) **306**, 456 (1983).
[47] P. Basera, A. Singh, D. Gill, and S. Bhattacharya, J. Mater. Chem. C **9**, 17113 (2021).
[48] R. A. Kerner and B. P. Rand, J. Phys. Chem. Lett. **9**, 132 (2018).